

Part of Topical Section on
Advanced Concepts in Silicon Based Photovoltaics

Hydrogen related phenomena at the ITO/a-Si:H/Si heterojunction solar cell interfaces

Alexander Ulyashin^{*1} and Anna Sytchkova^{**2}

¹ SINTEF Materials and Chemistry, Forskningsveien 1, P.O. Box 124, 0314 Oslo, Norway

² Optical Coatings Laboratory, ENEA Casaccia C.R.E., Via Anguillarese 301, 00123 Rome, Italy

Received 9 July 2012, revised 17 September 2012, accepted 22 September 2012

Published online 00 Month 2012

Keywords AFM, heterojunctions, hydrogen, ITO, silicon, SSRM

* Corresponding author: e-mail alexander.g.ulyashin@sintef.no, Phone: +47 9300 2224, Fax: +47 2206 7926

** e-mail anna.sytchkova@enea.it, Phone: +39 06 3048 4441, Fax: +39 06 3048 6364

Properties of thin a-Si:H and indium-tin oxide (ITO) layers as well as properties of interfaces of Si based heterojunction (HJ) ITO/(p)a-Si:H/n-Si structures were analyzed by means of atomic force microscopy (AFM) and scanning spreading resistance microscopy. It is shown that the morphology of thin ITO layers grown on n-type polished crystalline Si or on (p)a-Si:H/n-Si substrates depends on the deposition temperature and has peculiarities on a nano-scale. Formation of highly conductive nano-dots on the surface and in the bulk of ITO layers is found. The observed nano-spots and nano-dots are attributed to the influence of hydrogen initiated reduction process, which occurs upon deposition of ITO films on an

a-Si:H layer during the fabrication process of a HJ solar cell. This fact is confirmed by investigation of morphological properties of ITO surfaces after treatment by hydrogen plasma. It is shown that formation of conductive nano-particles on the ITO surface initiated by hydrogen does not change essentially transparency of an ITO layer. It is concluded that conductive nano-dots at the ITO/a-Si:H interface can be considered as local conductive channels, which provide a current flow through the ITO/(p)a-Si:H interface without essential shadowing of the solar cell structure. This finding opens an interesting way for the optimization of properties of the ITO/Si-based HJ solar cells.

© 2012 WILEY-VCH Verlag GmbH & Co. KGaA, Weinheim

1 Introduction Investigations of Si based heterojunction (HJ) solar cells, which consist of transparent conductive oxide (TCO)/Si structures started a long time ago [1–6] and are still intensive nowadays [7]. Such solar cells are regarded as low-cost photovoltaic devices. The cost reduction is provided by the low-temperature junction-formation step and by the unique properties of the TCO layer, which serves as an emitter, a conductive top electrode and as an antireflection coating. A remarkable progress for such solar cells has been demonstrated by SANYO [8] using an a-Si:H as an emitter as well as a buffer layer between the TCO top electrode and the Si substrate. Nevertheless, a number of problems in this field still remain unsolved [7, 9]. In particular, it is not clear so far why the efficiency of such solar cells is higher for n-type substrates than for p-type ones, and this represents a subject for intensive investigations [9–11]. It is interesting to note that this problem has been discussed earlier with regard to the TCO/Si solar cell efficiency. It was found that in many cases only n-type silicon substrates could provide fabrication of high-

efficiency HJ solar cells [6]. It was established that peculiarities of the interfaces between the TCOs, such as indium-tin oxide (ITO), and the Si substrate are responsible for this phenomenon. These peculiarities were attributed to the formation of defects on the ITO/Si interface since the TCO layer growth, which is usually done by a magnetron sputtering, leads to formation of ion damages in the Si subsurface region of the Si substrate. These damages induce a positive charge decreasing the surface barrier height in the case of n-type Si, while increasing the barrier in the case of p-type Si [12]. The interface properties of TCO/Si structures have been intensively studied in the past [13] and recently [14, 15] by means of current- and capacitance–voltage measurements. However, because of nano-size dimensions of the ITO (70–80 nm) and a-Si:H (3–20 nm) layers in ITO/Si and ITO/a-Si:H/Si solar cells these structures have to be investigated by atomic force microscopy (AFM) and scanning spreading resistance microscopy (SSRM) methods, as it was demonstrated in [16, 17]. It is worth noting that these analytical methods are widely used for nano-size systems

1 and it is reasonable to apply them for Si-based HJ solar cell
2 structures for characterization in addition to the conventional
3 electrical methods. The goal of this work is to investigate the
4 properties of ITO/n-Si and ITO/(p)a-Si:H/n-Si structures and
5 in particular, the interfaces in these structures on nano-scale,
6 by means of AFM and SSRM methods.

7 **2 Experimental details** Polished (100)-oriented
8 n-type Si wafers were used as substrates for the fabrication
9 of ITO/(p)a-Si:H/n-Si HJ structures. Prior deposition of
10 a-Si:H layer to all Si substrates the standard RCA cleaning
11 has been applied.

12 The 5 nm thick p-type a-Si:H layers were deposited in
13 the “p-chamber” of a plasma enhanced chemical vapor
14 deposition (PECVD) set up at following process conditions:
15 13.56 MHz frequency, 4.3 W power, 106.4 Pa (800 mTorr)
16 deposition pressure, $\sim 200^\circ\text{C}$ deposition temperature,
17 40 sccm flow rate for SiH₄ and 10 sccm for 2% mixture of
18 trimethylboron in He.

19 The ITO layers with thicknesses of 70–80 nm were
20 deposited at room temperature (RT), 160 and at 230°C
21 (substrate temperatures) using an ITO sintered target, with
22 In₂O₃ and SnO₂ in a weight proportion of 9:1. The DC
23 plasma power was 100 W at all deposition temperatures. The
24 base pressure in the sputter system was about 1.33 Pa (10–
25 5 Torr). The total pressure of the sputtering gas mixture was
26 adjusted to 0.399 Pa (3 mTorr) during the film preparation.
27 The argon flow rate was kept constant at 38 sccm.

28 The AFM and SSRM measurements were performed
29 using a Digital Instrument’s Nanoscope Dim 3100 micro-
30 scope equipped with spreading resistance and capacitance
31 measurement electronics. The AFM measurements were
32 performed in tapping mode using commercial silicon tips
33 MikroMasch NSC35/AIBS with a typical tip curvature
34 radius of less than 10 nm. The following parameters were
35 used for the analysis of the AFM measurements: (i) the root
36 mean square (RMS) roughness (R_q), which gives the root
37 mean square average of height deviations taken from the
38 mean data plane within a given area; (ii) the mean roughness
39 (R_a), which represents the arithmetic average of the absolute
40 values of the surface height deviations measured from the
41 mean plane; (iii) the difference in height between the highest
42 and lowest points on the surface relative to the mean plane
43 (h_{\max}); (iv) the average differences of heights (h_{aver}) [18].

44 The SSRM measurements were performed using com-
45 mercial conductive B-doped diamond coated silicon tips
46 NanoSensors CDT/NCHR with a microscopic tip radius of
47 10 nm (on nano-roughness). A DC bias was applied to the tip
48 and the current flowing through the sample was measured by
49 a logarithmic current amplifier. The SSRM measurements
50 for ITO/a-Si:H/Si structures were performed in a “cross-
51 section” configuration: one electrode has been made on the
52 back side of the solar cell structure and the conductive tip was
53 used to perform mapping of the ITO surface conductivity.
54 Thus, the vertical current through the ITO/a-Si:H/Si
55 structure was measured in this case. In case of ITO/glass
56 structure, one electrode was made on the ITO surface and the

1 conductive tip of the SSRM system (second electrode) was
2 measuring the lateral current distribution.

3 To investigate the influence of atomic hydrogen on the
4 properties of the ITO layers, sample hydrogenation was
5 performed in the PECVD setup at 230°C for 2 min using a
6 110 MHz plasma generator. The RF plasma density was
7 0.04 W cm^{-2} during the hydrogenation process, while the
8 ignition of plasma was done at higher densities (above
9 0.1 W cm^{-2}). At the stage of the plasma ignition the samples
10 were removed from the plasma area and then reintroduced
11 once the discharge had been stabilized at the density of
12 0.04 W cm^{-2} with the hydrogen gas flux of 200 sccm.

13 Direct transmittance of ITO glass samples was measured
14 in the spectral range of 250–3300 nm with a UV/VIS/NIR
15 double channel spectrophotometer (Perkin Elmer Lambda
16 950).

17 **3 Results and discussions** Figure 1 shows the sur-
18 face morphology (3D AFM image) of (p)a-Si:H layers
19 deposited on (100) oriented Si substrate at a temperature
20 about 200°C . From Fig. 1 it can be concluded that the a-Si:H
21 layer is rather flat on nano-scale, without any specific
22 morphological peculiarities.

23 Figure 2 shows the surface morphology of ITO layers
24 deposited on (p)a-Si:H/n-Si substrates at RT (Fig. 3a),
25 160°C (Fig. 3b) and 230°C (Fig. 3c).

26 From these images one may conclude that the roughness
27 of ITO layers deposited at 160 and 230°C on a hydrogen
28 containing a-Si:H layer is higher than for the case of the
29 RT deposition. This means that the morphology of ITO
30 layers, as well as other properties, depend substantially on
31 the deposition temperature, as it was reported in [16, 20]
32 for similar ITO layers deposited by magnetron sputtering on
33 Si and glass substrates at different temperatures [19].
34 Important to note that trends for ITO/glass structures are
35 different: the surface roughness of ITO layers decreases with
36 increasing of the deposition temperature [19].

37 Figure 3a shows the SSRM image of the ITO (RT)/(p)a-
38 Si:H/n-Si surface.

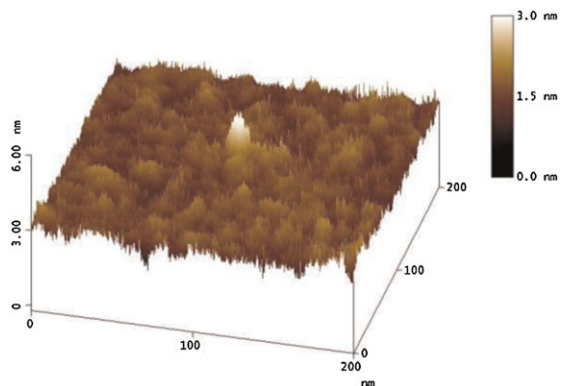


Figure 1 (online color at: www.pss-a.com) AFM 3D image of (p)a-Si:H layer deposited at $\sim 200^\circ\text{C}$ on an n-type polished Si substrate ($R_q = 0.164\text{ nm}$, $R_a = 0.129\text{ nm}$, $h_{\max} = 1.741\text{ nm}$, $h_{\text{aver}} = 0.7\text{ nm}$).

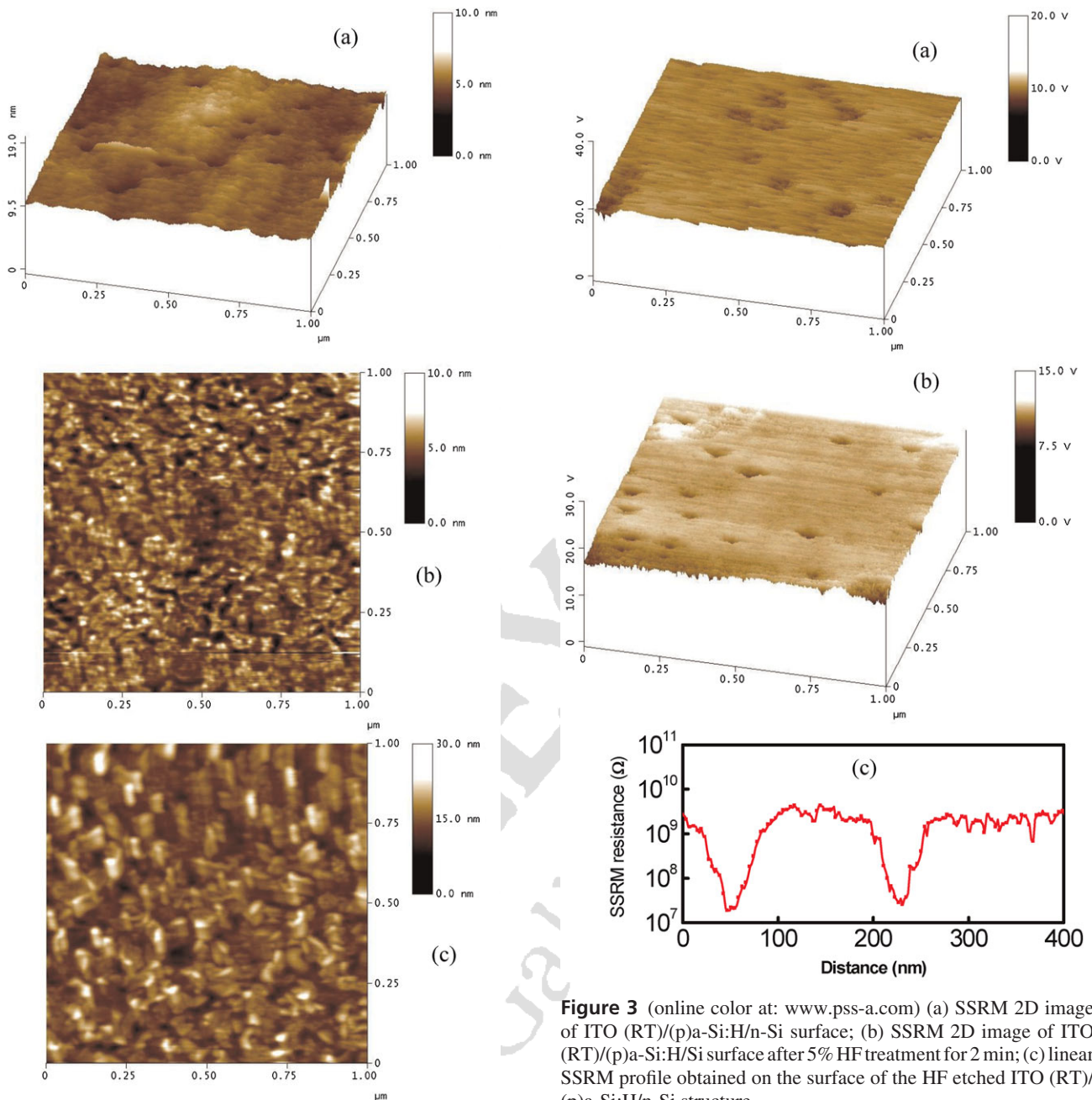


Figure 2 (online color at: www.pss-a.com) AFM 3D image of ITO layer deposited on (p)a-Si:H/n-Si substrate at (a) RT ($R_q = 0.29$ nm, $R_a = 0.23$ nm, $h_{max} = 3.6$ nm, $h_{aver} = 1.3$ nm); (b) 2D images of ITO layer deposited at 160 °C ($R_q = 1.0$ nm, $R_a = 0.74$ nm, $h_{max} = 30$ nm, $h_{aver} = 11.3$ nm); and (c) 230 °C ($R_q = 3.12$ nm, $R_a = 2.43$ nm, $h_{max} = 22$ nm, $h_{aver} = 14.6$ nm).

Figure 3 (online color at: www.pss-a.com) (a) SSRM 2D image of ITO (RT)/(p)a-Si:H/n-Si surface; (b) SSRM 2D image of ITO (RT)/(p)a-Si:H/n-Si surface after 5% HF treatment for 2 min; (c) linear SSRM profile obtained on the surface of the HF etched ITO (RT)/(p)a-Si:H/n-Si structure.

SSRM image correspond to local regions with lower resistance. It is interesting to note that these highly conductive nano-dots remain after etching of the ITO layers by 5% HF (Fig. 3b). AFM measurements for etched samples show similar morphology as for a-Si:H/n-Si structures (Fig. 1), which indicates that ITO layer has been removed completely by the HF etching. The linear spreading resistance profile shown in Fig. 3c indicates that the difference in absolute values of the spreading resistance for different local regions may be as large as two orders of magnitude, approximately. Therefore, it can be concluded that these highly conductive

1 A DC forward bias of 0.1 V was applied to the tip and
2 the current flowing through the sample was measured by a
3 logarithmic current amplifier.

4 The SSRM data are presented using a voltage scale, and
5 can be converted by a standard procedure to the spreading
6 resistance values [18]. Darker spots (nano-dots) on the

1 local regions provide a current flow through the conductive
2 nano-channels at the ITO/(p)a-Si:H interface. Nevertheless
3 it has to be noted that at this stage it is not clear how the
4 observed highly conductive channels have been formed.
5 The following scenario can be considered, as the most
6 probable version: metallic rich clusters with high conductivity
7 can be formed at the initial stage of the ITO growth
8 on top of an a-Si:H layer due to reduction process initiated
9 by hydrogen, released from the a-Si:H layer. Independently
10 on the reasons, which lead to the formation of such
11 conductive local regions at the ITO/Si interfaces, it can be
12 stated that properties of these conductive nano-channels
13 (size, density, conductivity, etc.) are very probably crucial
14 for the properties of Si based HJ solar cells. The validity of
15 this conclusion should be verified by a more detailed
16 examination of the nano-scale properties of ITO/a-Si:H/Si
17 structures. Such analysis is ultimately necessary and
18 extremely important in this case, since conventional
19 techniques like DLTS or CV methods have limited spatial
20 resolution.

21 It has to be noted that in [9] it was demonstrated that a
22 release of hydrogen from the a-Si:H layer occurs during the
23 ITO deposition process. It can be assumed that the hydrogen
24 release could be responsible for the observed morphological
25 peculiarities due to ability of hydrogen to initiate reduction
26 processes for any oxides.

27 In order to prove that hydrogen can affect properties of
28 thin ITO layers, a flat 80 nm thick ITO layer was deposited on
29 a glass substrate at 230 °C, and subsequently hydrogenated at
30 230 °C for 2 min.

31 Figure 4a shows 2D images for ITO (230 °C)/glass
32 structure before and after (Fig. 4b) the hydrogen plasma
33 treatment at 230 °C for 2 min. Important to note that ITO
34 layer deposited at 230 °C is rather flat and any changes of the
35 morphology for such layers can be detected easy. From
36 Fig. 4b it can be seen that formation of nano-structures
37 occurs as fast as after just 2 min of hydrogenation with a
38 power density as low as 0.04 W cm⁻²; the structures have a
39 typical size of 20–40 nm with a tendency to agglomerate.
40 From Fig. 4 it can be concluded that hydrogen plasma
41 treatment causes remarkable changes in the morphology of
42 ITO layer, even for rather short times of the oxide reduction
43 process, which can be performed at rather low (230 °C)
44 temperatures.

45 Figure 5a shows the SSRM 2D image obtained for
46 the ITO (230 °C)/glass structure after a hydrogen plasma
47 treatment at 230 °C for 2 min.

48 The SSRM measurements were done with a dc bias of
49 –0.1 V applied to the tip, and the results of the SSRM
50 mapping are shown in terms of voltage scale where darker
51 regions correspond to higher conductivity values.

52 To correlate the spatial variation of the conductivity with
53 topography, a linear SSRM scan with simultaneous data
54 acquisition was performed (Fig. 5b). To ensure reproducibility
55 of the measurement results and their stability against
56 the topography induced noise, both trace and retrace scans
57 were performed. Further, the SSRM data acquired in the

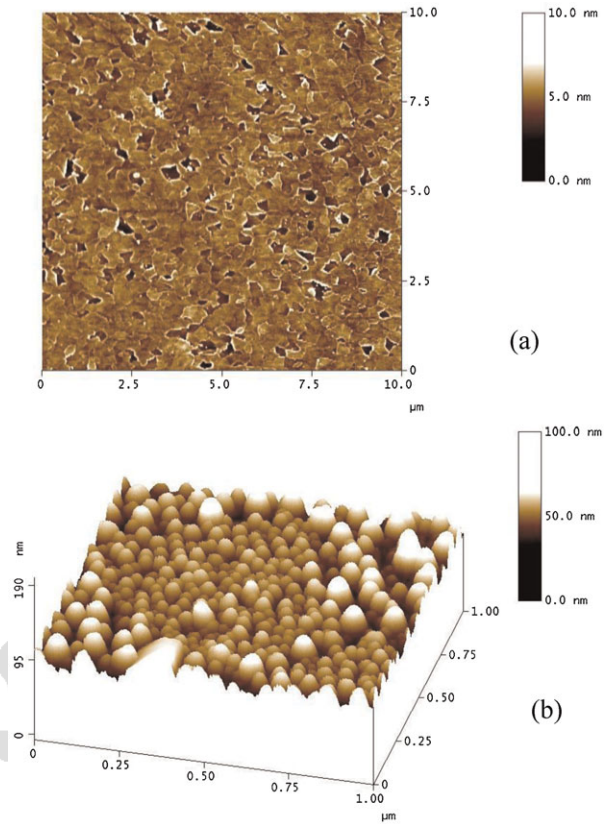


Figure 4 (online color at: www.pss-a.com) AFM images of ITO (230 °C)/glass structures: (a) – before, and (b) – after hydrogen plasma treatment at 230 °C for 2 min.

voltage scale used by the software of the Digital Instrument's
Nanoscope Dim 3100 system were converted into SSRM
resistance via a standard procedure described in [18]. From
Fig. 5b it is seen that the morphology and the resistance
do not exhibit a clear correlation. In some cases the
maximum height corresponds to the maximum value of
the resistance while in other cases the opposite behavior
can be observed.

Thus, all nano-structures do not have maximum
conductivity at their maximum heights. This indicates
that the composition of the observed nano-structures at
the initial stages of their formation is not fully metallic
and probably consists of partially reduced oxides with
high resistivity. Nevertheless, highly conductive nano-
structures are clearly revealed from Fig. 5b, and the
difference in the spreading resistance can be as high as 5
orders of magnitude, approximately. It should be noted
that for the untreated ITO (230 °C)/glass structures, local
deviations of the conductivity do not exceed one order
of magnitude. The “macroscopic” resistivity of such ITO
layer before hydrogenation measured by conventional four
probe method is about $2.7 \times 10^{-4} \Omega \text{ cm}$. After hydrogen-
ation the resistivity is almost un-changed and shows a bit
better value $\sim 2.3 \times 10^{-4} \Omega \text{ cm}$.

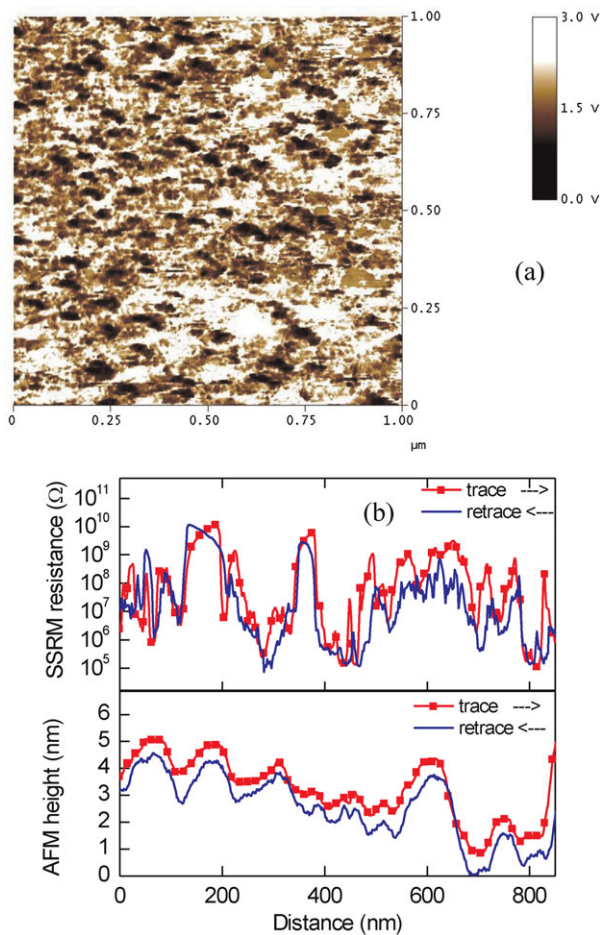


Figure 5 (online color at: www.pss-a.com) SSRM images of ITO (230 °C)/glass structures. (a) – before and (b) – after hydrogen plasma treatment at 230 °C for 2 min. Linear SSRM profile taken at an arbitrary position not indicated on the SSRM mapping image. For SSRM measurements DC bias used was -0.1 V.

Important to note that the lateral current flow in ITO/glass structure after hydrogen plasma treatment is not homogeneous, and show similar peculiarities as in case of ITO/a-Si:H structures – formation of local highly conductive regions/channels.

It can be concluded that morphological and electrical properties ITO layers can be easily modified by atomic hydrogen, which is present in hydrogen plasma. Therefore, it can be assumed that similar processes occur at the ITO/a-Si:H interface upon deposition of ITO layer since atomic hydrogen can be released from an a-Si:H layer upon deposition of ITO on an a-Si:H/Si substrate. Important to note with this regards that hydrogen release from the a-Si:H layer upon ITO deposition is a well established fact, which has been presented in [10]. Thus, although we are considering our explanation concerning the formation of highly conductive regions at the ITO/a-Si:H interfaces as an assumption, this assumption has rather solid background from our point of view.

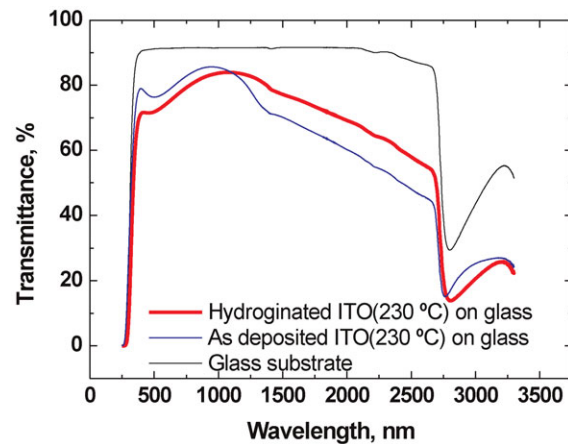


Figure 6 (online color at: www.pss-a.com) Transmittance of ITO (230 °C)/glass structure after hydrogen plasma treatment at 230 °C for 2 min.

Transmittance of ITO (230 °C)/glass structure after hydrogen plasma treatment at 230 °C for 2 min is shown in Fig. 6.

Figure 6 illustrates that despite the formation of nanoparticles on the ITO surface initiated by hydrogen, such plasma-treated layer is sufficiently transparent to be used as a transparent front side electrode and at the same time as an antireflection coating for solar cells: it has more than 80% transmittance in the visible spectral range and its transmittance is even improved in the near IR, compared to that of as deposited ITO film.

4 Conclusions The AFM measurement study performed in this work has demonstrated that the morphology of thin ITO layers grown on n-type polished crystalline Si or on (p)a-Si:H/n-Si substrates depends on the deposition temperature and has peculiarities on nano-scale. Formation of nano-wells, which can be attributed to a hydrogen initiated reduction process of ITO in local regions during the ITO deposition process, is observed on the ITO surface in ITO/a-Si:H/Si structures.

Moreover, formation of highly conductive nano-dots/channels on the surface of ITO layers has been observed. These local regions provide current flow through the conductive nano-channels at the ITO/(p)a-Si:H interface.

It is necessary to underline that formation of conductive channels can be attributed to the peculiarities at the ITO/a-Si:H interface, since channels have been observed (SSRM mapping) on ITO or ITO etched surfaces of HJ ITO/a-Si:H structures. Similar peculiarities have been observed for the ITO/glass structures, after hydrogen plasma treatments, which shows that hydrogen initiated ITO structure modification is responsible for the formation of highly conductive in ITO structures.

Therefore, it is supposed that formation of highly conductive nano-channels occurs due to hydrogen initiated reduction process at the initial stage of ITO films formation

1 in the case of magnetron sputtering on a-Si:H layers. This
2 assumption is supported by investigations of morphological
3 and electrical properties of ITO surfaces in ITO/glass after
4 treatment by hydrogen plasma, which shows that indeed,
5 highly conductive channels in ITO layers can be formed in
6 presence of the atomic hydrogen. Nevertheless, important to
7 note, that the proposed explanation is only an assumption,
8 which has to be verified by further studies of ITO/a-Si:H
9 interfaces on nano-scale.

10 It has been found that nano-structure formation on ITO
11 surface occurs at hydrogenation temperatures as low as
12 230 °C and as fast as for only 2 min. Formation of conductive
13 nano-particles on the ITO surface initiated by hydrogen
14 does not change essentially their transparency, and such
15 treated ITO layer can be used as a transparent front side
16 electrode and at the same time as antireflection coating for
17 solar cells.

18 To optimize properties of ITO/a-Si:H/Si HJ solar cells,
19 an adequate control of such local conductive channels
20 formation should be guaranteed during solar cell fabrication.

21 **Acknowledgements** The authors gratefully acknowledge
22 Kestys Maknys for technical support with SSRM measurements.

23 References

24 [1] K. Kajiyama and Y. Furukawa, *Jpn. J. Appl. Phys.* **6**, 905 (1967).
25 [2] T. Nishino and Y. Hamakawa, *Jpn. J. Appl. Phys.* **9**, 1085 (1970).
26 [3] R. L. Andersen, *Appl. Phys. Lett.* **27**, 691 (1975).
27 [4] S. J. Fonash, *J. Appl. Phys.* **46**, 1286 (1975).
28 [5] A. K. Gnosh, C. Fishman, and T. Feng, *J. Appl. Phys.* **49**,
29 3490 (1978).
30 [6] T. Feng, A. Gnosh, and C. Fishman, *J. Appl. Phys.* **50**, 4972
31 (1979).
32 [7] F. Roca, J. Carabe, and A. Jager-Waldau, in: 19th European
33 Photovoltaic Solar Energy Conference, Vol. II, edited by
34 W. Hoffmann, J.-L. Bal, H. Ossenbrink, W. Palz, and P. Helm
35 (WIP, Munich; ETA, Florence, 2004) p. 1321.

[8] M. Taguchi, K. Kawamoto, S. Tsuge, T. Baba, H. Sakata,
1 M. Morizane, K. Uchihashi, N. Nakamura, S. Kiyama, and
2 O. Oota, *Prog. Photovolt.* **8**, 503 (2000). 3
[9] A. Ulyashin, R. Bilyalov, L. Carnel, K. Van Nieuwenhuysen,
4 D. Grambole, A. Bruck, M. Scherff, E. Monakhov, A. Yu.
5 Kuznetsov, B. G. Svensson, G. Beaucarne, and J. Poortmans,
6 in: 19th European Photovoltaic Solar Energy Conference,
7 Vol. I, edited by W. Hoffmann, J.-L. Bal, H. Ossenbrink,
8 W. Palz, and P. Helm (WIP, Munich; ETA, Florence 2004)
9 p. 588. 10
[10] M. Scherff, A. Froitzheim, A. G. Ulyashin, M. Schmidt,
11 W. R. Fahrner, and W. Fuhs, in: [PV in Europe. From PV
12 Technology to Energy Solutions^{Q1}](#), Vol. I, edited by J. L. Bal,
13 G. Silvestrini, A. Grassi, W. Palz, R. Vigotti, M. Gamberale,
14 and P. Helm (2002) p. 216. 15
[11] M. Schmidt, L. Korte, K. Kliefoth, A. Schoepke, R. Stangl,
16 A. Laades, E. Conrad, K. Brendel, W. Fuhs, M. Scherff, and
17 W. Fahrner, in: 19th European Photovoltaic Solar Energy
18 Conference, Vol. I, edited by W. Hoffmann, J. L. Bal,
19 H. Ossenbrink, W. Palz, and P. Helm (WIP, Munich;
20 ETA, Florence, 2004) p. 592. 21
[12] S. Ashok, T. P. Chow, and B. J. Baliga, *Appl. Phys. Lett.* **42**,
22 687 (1983). 23
[13] S. Ashok, S. J. Fonash, R. Singh, and P. Wiley, *IEEE Electron
24 Device Lett.* **EDL-2**, 184 (1981). 25
[14] A. Froitzheim, K. Brendel, L. Elstner, W. Fuhs, K. Kliefoth,
26 and M. Schmidt, *J. Non-Cryst. Solids* **299–302**, 663 (2002). 27
[15] N. Jensen, U. Rau, R. M. Hausner, S. Uppal, L. Oberbeck, and
28 R. B. Bergmann, *J. Appl. Phys.* **87**, 2639 (2000). 29
[16] K. Maknys, A. G. Ulyashin, A. Yu. Kuznetsov, and B. G.
30 Svensson, *Thin Solid Films* **511–512**, 98 (2006). 31
[17] J. S. Christensen, A. G. Ulyashin, A. Yu. Kuznetsov, and
32 B. G. Svensson, *Thin Solid Films* **511–512**, 93, (2006). 33
[18] *Electrical Application Modules: Dimension and MultiMode*,
34 Veeco Instruments Inc. (2003). 35
[19] S. Diplas, A. Ulyashin, K. Maknys, A. E. Gunnaes, S. Jorgensen,
36 A. Olsen, and T. G. Finstad, *Thin Solid Films* **515**, 8539
37 (2007). 38
[20] A. V. Mudryi, A. V. Ivaniukovich, and A. G. Ulyashin, *Thin
39 Solid Films* **515**, 6489 (2007). 40

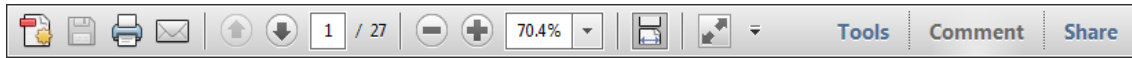
41 **Q1:** Author: Please provide the publisher and location.
42

USING e-ANNOTATION TOOLS FOR ELECTRONIC PROOF CORRECTION

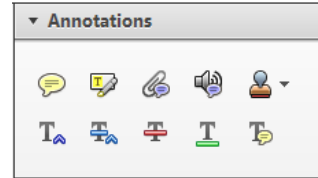
Required software to e-Annotate PDFs: **Adobe Acrobat Professional** or **Adobe Reader** (version 8.0 or above). (Note that this document uses screenshots from **Adobe Reader X**)

The latest version of Acrobat Reader can be downloaded for free at: <http://get.adobe.com/reader/>

Once you have Acrobat Reader open on your computer, click on the **Comment** tab at the right of the toolbar:



This will open up a panel down the right side of the document. The majority of tools you will use for annotating your proof will be in the **Annotations** section, pictured opposite. We've picked out some of these tools below:



1. Replace (Ins) Tool – for replacing text.

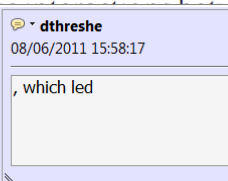


Strikes a line through text and opens up a text box where replacement text can be entered.

How to use it

- Highlight a word or sentence.
- Click on the **Replace (Ins)** icon in the Annotations section.
- Type the replacement text into the blue box that appears.

standard framework for the analysis of microeconomic activity. Nevertheless, it also led to the development of a number of strategic approaches. The number of competitors in an industry is that the structure of the industry is a main component of the competitive environment. At the firm level, are externalities an important part of the firm's cost structure? (M henceforth) we open the black b



2. Strikethrough (Del) Tool – for deleting text.



Strikes a red line through text that is to be deleted.

How to use it

- Highlight a word or sentence.
- Click on the **Strikethrough (Del)** icon in the Annotations section.

there is no room for extra profits as long as the number of firms is large enough. If the number of firms is small, the number of firms is determined by the number of firms. Blanchard and Kiyotaki (1987), in their paper on perfect competition in general equilibrium, show that the effects of aggregate demand and supply shocks in a classical framework assuming monopolistic competition are an exogenous number of firms

3. Add note to text Tool – for highlighting a section to be changed to bold or italic.



Highlights text in yellow and opens up a text box where comments can be entered.

How to use it

- Highlight the relevant section of text.
- Click on the **Add note to text** icon in the Annotations section.
- Type instruction on what should be changed regarding the text into the yellow box that appears.

dynamic responses of mark-ups to cost changes. The evidence is consistent with the VAR evidence

sation of the industry. The number of firms in the industry is a main component of the competitive environment. At the firm level, are externalities an important part of the firm's cost structure? (M henceforth) we open the black b



4. Add sticky note Tool – for making notes at specific points in the text.



Marks a point in the proof where a comment needs to be highlighted.

How to use it


- Click on the **Add sticky note** icon in the Annotations section.
- Click at the point in the proof where the comment should be inserted.
- Type the comment into the yellow box that appears.

and supply shocks. Most of the evidence is consistent with the VAR evidence. The number of firms in the industry is a main component of the competitive environment. At the firm level, are externalities an important part of the firm's cost structure? (M henceforth) we open the black b



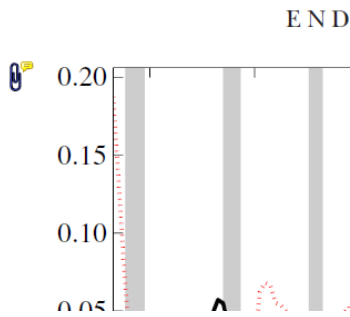
USING e-ANNOTATION TOOLS FOR ELECTRONIC PROOF CORRECTION

5. Attach File Tool – for inserting large amounts of text or replacement figures.


 Inserts an icon linking to the attached file in the appropriate place in the text.

How to use it

- Click on the **Attach File** icon in the Annotations section.
- Click on the proof to where you'd like the attached file to be linked.
- Select the file to be attached from your computer or network.
- Select the colour and type of icon that will appear in the proof. Click OK.

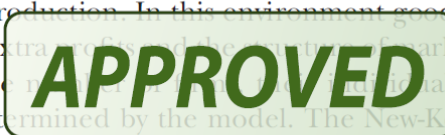


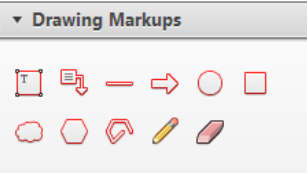
6. Add stamp Tool – for approving a proof if no corrections are required.

 Inserts a selected stamp onto an appropriate place in the proof.

How to use it

- Click on the **Add stamp** icon in the Annotations section.
- Select the stamp you want to use. (The **Approved** stamp is usually available directly in the menu that appears).
- Click on the proof where you'd like the stamp to appear. (Where a proof is to be approved as it is, this would normally be on the first page).

of the business cycle, starting with the
 on perfect competition, constant ret
 production. In this environment goods
 extra of the economy. The price of the
 he is the only one who can be
 determined by the model. The New-Key
 otaki (1987), has introduced produc
 general equilibrium models with nomin
 and...


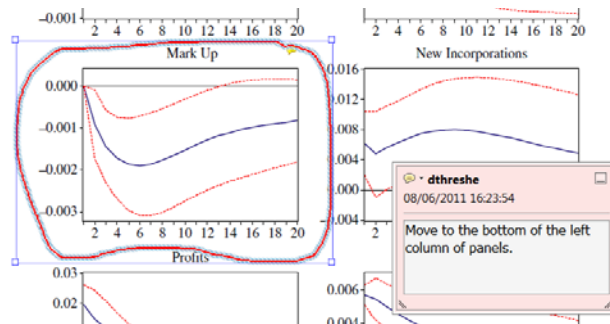


7. Drawing Markups Tools – for drawing shapes, lines and freeform annotations on proofs and commenting on these marks.

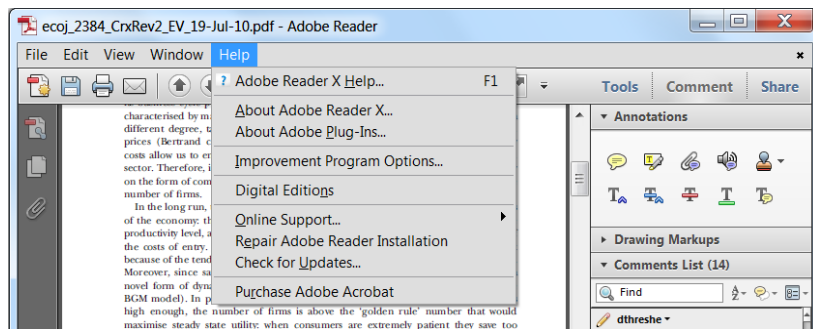
Allows shapes, lines and freeform annotations to be drawn on proofs and for comment to be made on these marks..

How to use it

- Click on one of the shapes in the **Drawing Markups** section.
- Click on the proof at the relevant point and draw the selected shape with the cursor.
- To add a comment to the drawn shape, move the cursor over the shape until an arrowhead appears.
- Double click on the shape and type any text in the red box that appears.



For further information on how to annotate proofs, click on the **Help** menu to reveal a list of further options:



Manuscript No.

Author/Title/Issue No.

Required Fields may be filled in using Acrobat Reader

Please correct your galley proofs and return them within 4 days together with the completed reprint order form. The editors reserve the right to publish your article with editors' corrections if your proofs do not arrive in time.

After having received your corrections, your paper will be published online up to several weeks ahead of the print edition in the EarlyView service of Wiley Online Library (wileyonlinelibrary.com).

Please keep in mind that reading proofs is your responsibility. Corrections should therefore be clear. The use of standard proof correction marks is recommended. Corrections listed in an electronic file should be sorted by line numbers.

LaTeX and Word files are sometimes slightly modified by the production department to follow general presentation rules of the journal.

Note that the quality of the halftone figures is not as high as the final version that will appear in the issue.

Check the enclosed galley proofs very carefully, paying particular attention to the formulas (including line breakings introduced in production), figures, numerical values, tabulated data and layout of the pages.

A black box (■) or a question at the end of the paper (after the references) signals unclear or missing information that specifically requires **your attention**. Note that the author is liable for damages arising from incorrect statements, including misprints.

The main aim of proofreading is to correct errors that may have occurred during the production process, **and not to modify the content of the paper**. Corrections that may lead to a change in the page layout should be avoided.

Note that sending back a corrected **manuscript file is of no use**.

If your paper contains **color figures**, please fill in the Color Print Authorization and note the further information given on the following pages. Clearly mark desired **color print figures** in your proof corrections.

Return the corrected proofs within 4 days by e-mail.

Please do not send your corrections to the typesetter but to the Editorial Office:

E-MAIL: pssa.proofs@wiley-vch.de

Please limit corrections to errors in the text; cost incurred for any further changes or additions will be charged to the author, unless such changes have been agreed upon by the editor.

Full color reprints, PDF files, Issues, Color Print, and Cover Posters may be ordered by filling out the accompanying form.

Contact the Editorial Office for **special offers** such as

- Personalized and customized reprints (e.g. with special cover, selected or all your articles published in Wiley-VCH journals)
- Cover/frontispiece publications and posters (standard or customized)
- Promotional packages accompanying your publication

Visit the **MaterialsViews.com Online Store** for a wide selection of posters, logos, prints and souvenirs from our top physics and materials science journals at www.cafepress.com/materialsviews

Order Form



2011 WILEY-BLACKWELL
WILEY-VCH GmbH & Co. KGaA
physica status solidi
Rotherstrasse 21
10245 Berlin
Germany
TEL +49 (0) 30 47 03 13 31
FAX +49 (0) 30-47 03 13 34
E-MAIL pssa.proofs@wiley-vch.de

Please complete this form and return it by FAX or e-mail.

Manuscript No.

Author/Title/Issue No.

Required Fields may be filled in using Acrobat Reader

Reprints/Issues/PDF Files/Posters

Whole issues, reprints and PDF files (300 dpi) for an unlimited number of printouts are available at the rates given on the third page. Reprints and PDF files can be ordered before *and after* publication of an article. All reprints will be delivered in full color, regardless of black/white printing in the journal.

Reprints

Please send me and bill me for

- full color reprints with color cover
 full color reprints with color cover **and** customized color sheet

Issues

Please send me and bill me for

- entire issues

PDF

Please send me and bill me for

- a PDF file (300 dpi) for an unlimited number of printouts **with customized cover sheet.**

The PDF file will be sent to your e-mail address.

Send PDF file to:

Please note that posting of the final published version on the open internet is not permitted. For author rights and re-use options, see the Copyright Transfer Agreement at <http://www.wiley.com/go/ctavchglobal>.

Cover Posters

Posters are available of all the published covers in two sizes (see attached price list). **Please send me and bill me for**

- A2 (42 × 60 cm/17 × 24in) posters
 A1 (60 × 84 cm/24 × 33in) posters

Mail reprints and/or issues and/or posters to (no P.O. Boxes):

Color print authorization

Please bill me for

- color print figures (total number of color figures)
 YES, please print Figs. No. in color.
 NO, please print all color figures in black/white.

VAT number:

Tax-free charging can only be processed with the VAT number of the institute/company. To prevent delays, please provide us with the VAT number with this order.

Purchase Order No.:

Terms of payment:

- Please send an invoice Cheque is enclosed
Please charge my credit card



Expiry date

Card no.	<input type="text"/>
Card Verification Code	<input type="text"/>

Date, Signature _____

Send bill to:

Signature _____

Date _____

Subscriptions

For ordering information, claims and any enquiry concerning your journal subscription please go to www.wileycustomerhelp.com or contact your nearest office.

Americas: e-mail: cs-journals@wiley.com; Tel: +1 781 388 8598 or +1 800 835 6770 (toll free in the USA & Canada)

Europe, Middle East and Africa: e-mail: cs-journals@wiley.com; Tel: +44 (0) 1865 778315.

Asia Pacific: e-mail: cs-journals@wiley.com; Tel: +65 6511 8000.

Japan: For Japanese speaking support, e-mail: cs-japan@wiley.com; Tel: +65 6511 8010 or Tel (toll-free): 005 316 50 480.

Price List for Reprints 2011 – pss (a)

The prices listed below are valid only for orders received in the course of 2011. Minimum order is 50 copies.

Reprints can be ordered before and after publication of an article. All reprints are delivered with color cover and color figures. If more than 500 copies are ordered, special prices are available upon request.

Single issues are available to authors at a reduced price.

The prices include mailing and handling charges. All prices are subject to local VAT/sales tax.

Reprints with color cover Size (pages)	Price for orders of (in Euro)					
	50 copies	100 copies	150 copies	200 copies	300 copies	500 copies*
1–4	330,—	385,—	425,—	445,—	548,—	752,—
5–8	470,—	556,—	608,—	636,—	784,—	1077,—
9–12	610,—	717,—	786,—	824,—	1016,—	1396,—
13–16	744,—	874,—	958,—	1004,—	1237,—	1701,—
17–20	885,—	1040,—	1138,—	1196,—	1489,—	2022,—
for every additional 4 pages	140,—	164,—	175,—	188,—	231,—	315,—
for additional customized colored cover sheet	190,—	340,—	440,—	650,—	840,—	990,—
PDF file (300 dpi, unlimited number of printouts, customized cover sheet) € 330.00						
Issues	€ 48.00 per copy for up to 10 copies.*					
Cover Posters	• A2 (42×60 cm/17×24in) € 49.00					
	• A1 (60×84 cm/24×33in) € 69.00					

*Prices for more copies available on request.

Special offer: If you order 100 or more reprints you will receive a pdf file (300 dpi, unlimited number of printouts, color figures) and an issue for free.

Color figures

If your paper contains **color figures**, please notice that, generally, these figures will appear in color in the online PDF version and all reprints of your article at no cost. This will be indicated by a note „(online color at: www.pss-a.com)“ in the caption. The print version of the figures in the journal hardcopy will be black/white unless the author explicitly requests a color print publication and contributes to the additional printing costs.

Approximate color print figure charges	
First figure	€ 495.00
Each additional figure	€ 395.00 Special prices for more color print figures on request

If you wish color figures in print, please answer the **color print authorization** questions on the second page of our Order Form and clearly mark the desired color print figures in your proof corrections.

Information regarding VAT:

Please note that for German sales tax purposes the charge for *color print* is considered a service and therefore is subject to German sales tax. For **institutional** customers in other countries the tax will be waived, i.e. the Recipient of Service is liable for VAT. Members of the EU will have to present a VAT identification number. Customers in other countries may also be asked to provide according tax identification information.